Showcasing research from the State Key Laboratory of Digital Manufacturing Equipment and Technology, Huazhong University of Science and Technology, Wuhan, China.

Title: Electrohydrodynamic direct-writing

The electrohydrodynamic (EHD) direct-writing technique can be used to print solid/liquid, straight/serpentine nanofibers onto a large-area substrate, in a direct, continuous and controllable manner, and is becoming a high-efficiency and cost-effective solution-processable technique to satisfy the increasing demands of large-area micro/nano-manufacturing. It is ground-breaking to direct-write sub-100-nm fibers using organic materials, combining dip-pen, inkjet, and electrospinning for sub-100 nm nanofabrication; and this overcomes the drawbacks of conventional electron-beam lithography which is relatively slow, complicated and expensive.

As featured in:

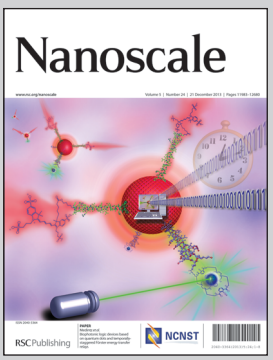

See Huang, Yin *et al.*, *Nanoscale*, 2013, **5**, 12007.

RSC Publishing

www.rsc.org/nanoscale

Registered Charity Number 207890

Nanoscale

RSC Publishing

REVIEW

View Article Online
View Journal | View Issue

Electrohydrodynamic direct-writing

Cite this: *Nanoscale*, 2013, **5**, 12007

YongAn Huang,* Ningbin Bu, Yongqing Duan, Yanqiao Pan, Huimin Liu, Zhouping Yin* and Youlun Xiong

The electrohydrodynamic (EHD) direct-writing technique can be used to print solid/liquid straight/serpentine nanofibers onto a large-area substrate, in a direct, continuous, and controllable manner. It is a high-efficiency and cost-effective solution-processable technique to satisfy increasing demands of large-area micro/nano-manufacturing. It is ground-breaking to direct-write sub-100 nm fibers on a rigid/flexible substrate using organic materials. A comprehensive review is presented on the research and developments related to the EHD direct-writing technique and print heads. Many developments have been presented to improve the controllability of the electrospun fibers to form high-resolution patterns and devices. EHD direct-writing is characterized by its non-contact, additive and reproducible processing, high resolution, and compatibility with organic materials. It combines dip-pen, inkjet, and electrospinning by providing the feasibility of controllable electrospinning for sub-100 nm nanofabrication, and overcomes the drawbacks of conventional electron-beam lithography, which is relatively slow, complicated and expensive.

Received 15th August 2013
Accepted 21st August 2013

DOI: 10.1039/c3nr04329k

www.rsc.org/nanoscale

Introduction

Organic materials can offer a low-cost alternative for printed and flexible electronics, such as flexible displays, electronic skin and large-area sensors.[1] Fabrication of these systems must exploit the differences, such as process simplicity, cost-effectiveness and environmental friendliness, and noncompatibility with high temperature processes, compared with traditional inorganic electronics, if they are to become commercially viable. Expensive and complicated multistep lithography processes may be avoided because they will damage organic materials and flexible substrates. Inkjet printing is an attractive method for producing electronic devices, on account of its minimal waste generation and efficient handling of expensive materials. A number of inkjet printers based on different actuation mechanisms, like thermal, piezoelectric and aerosol, *etc.* are commercialized and widely used in the electronic industry, however, the droplet size is usually 1.89 times larger than the nozzle diameter.[2] It leads to various intrinsic problems of nozzle blockage by high viscosity solution, overheating of organic materials and limited resolution in these existing printing devices, therefore a new direct-writing process based on electrohydrodynamics is the focal point of research.

The EHD direct-writing process pulls the fluids rather than pushes them like conventional inkjet printing processes; thus it offers a unique feature of generating a sub-100 nm jet or droplet, even smaller than one thousandth of the nozzle orifice.[3,4] EHD direct-writing is characterized by its high resolution, non-contact, additive and reproducible processing, and compatibility with high concentration organic/polymer solutions, and capability of depositing fibers onto silicon or polymer substrates directly.[3–8] It is rooted in traditional electrospinning, which, as an electrostatic fiber fabrication technique, has evinced increasing interest and attention, due to its versatility for producing ultra-thin fibers of nearly one hundred different materials, with diameters ranging from several micrometers down to a few nanometers.[1,9,10] The traditional electrospinning process is restricted to applications without the requirement of orderly patterns, because the chaotic nature of electrospinning seems incompatible with the patterned devices. A great deal of effort has been made in direct-writing isolated electrospun fibers, significantly expanding to the fabrication of micro/nano-devices, including electronic components and sacrificial or masking structures for nanofabrication purposes. For instance, positioned electrospun fibers act as physical biomimetic structures within lab-on-a-chip applications,[11] conductive nanofibers in field-effect transistors,[12] a nanowire electronic device,[13,14] a sacrificial layer for nanochannel fabrication,[15,16] and micro/nanofiber-shaped electronic devices.[17,18] Recently, considerable improvements have been made in the controllability on the positioning and morphology of fibers, to generate more elaborate micro/nanostructures.[19,20] EHD direct-writing simplifies the technique process, improves device performance, and reduces the fabrication cost. We are expecting this review to pave the way for fabrication of high performance organic electronics in a cost-effective and ingenious nanomanufacturing.

State Key Laboratory of Digital Manufacturing Equipment and Technology, Huazhong University of Science and Technology, Wuhan 430074, People's Republic of China. E-mail: yahuang@hust.edu.cn; yinzhp@mail.hust.edu.cn

Development of electrospinning

A standard electrospinning system is simple in terms of apparatus, while the physics of the process is extremely complex. A hemispherical liquid drop at the tip of a capillary will be distorted into a Taylor cone and form a liquid jet in the presence of an external electric field[21] or centrifugal force,[22,23] and the electrified jet involves the rapid stretching and rapid solidification. The jet extends initially in a straight line for a certain distance, then suffers a catastrophic bending instability, followed by a looping and spiraling path with increasing circumference.[24] The formation of nanofibers is determined by operating parameters:[1,20,25–27] (1) *Material factors*: molecular weight,[28] concentration,[3,28] viscosity,[29] conductivity, permittivity surface tension, and the substrate surface. (2) *Process factors*: needle-to-collector distance,[3,8,28] nozzle layout,[30] auxiliary electrodes,[31] applied voltage,[3,28,29] flow rate, and velocity of collector.[4,25,32] (3) *Circumstance factors*: humidity,[33] temperature air,[34] or viscosity of liquid.[35]

The evolution of electrospinning experiences approximately four stages, as shown in Fig. 1: traditional electrospinning for fabrication of nonwoven nanofibers, electrospinning with assisted-electrode or dynamic collector for fiber assembly,[31] near-field electrospinning (NFES) with the capability of positioning the electrospun nanofibers,[8] and mechano-electrospinning (MES) for positioning the electrospun nanofibers and tuning the morphology of the nanofibers in one step.[32] Traditional electrospinning deposits fibers in a random nonwoven mat, making it impossible to produce single-fiber devices. Electrospinning with auxiliary electrodes[25] or a dynamic mechanical collector,[4,36] however, just aligns fibers, unable to control a single fiber. It is significant to manipulate a single fiber to fabricate structures and devices on the micro/nano-scale. The controllability gradually increases, which leads electrospinning from disordered fiber-fabrication to high-controllable direct-writing technology.

It is ground-breaking to increase the controllability of a single fibre by reducing needle-to-collector distance h from more than 10 cm to less than 1 cm. It becomes possible to control and manipulate a single electrospun fiber, including position, shape and morphology of the single fiber. h plays a critical role in determining the dynamic behavior of flying fibers and the fiber morphology.[28,32] Here, we classify electrospinning into far-field electrospinning ($h > h_{straight} + h_{whipping\_1}$), medium-field electrospinning ($h_{straight} < h < h_{straight} + h_{whipping\_1}$) and near-field electrospinning ($h < h_{straight}$) (Fig. 2), and the differences are listed in Table 1. In far-field electrospinning, an applied voltage of 10–50 kV is usually adopted between the

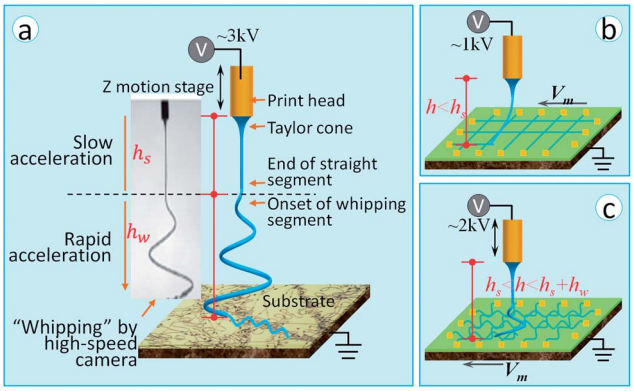

Fig. 2 (a) Standard electrospinning (far-field electrospinning) to fabricate a nonwoven mat. (b) Near-field electrospinning to direct-write fibers. (c) Medium-field electrospinning to deposit wavy structures.

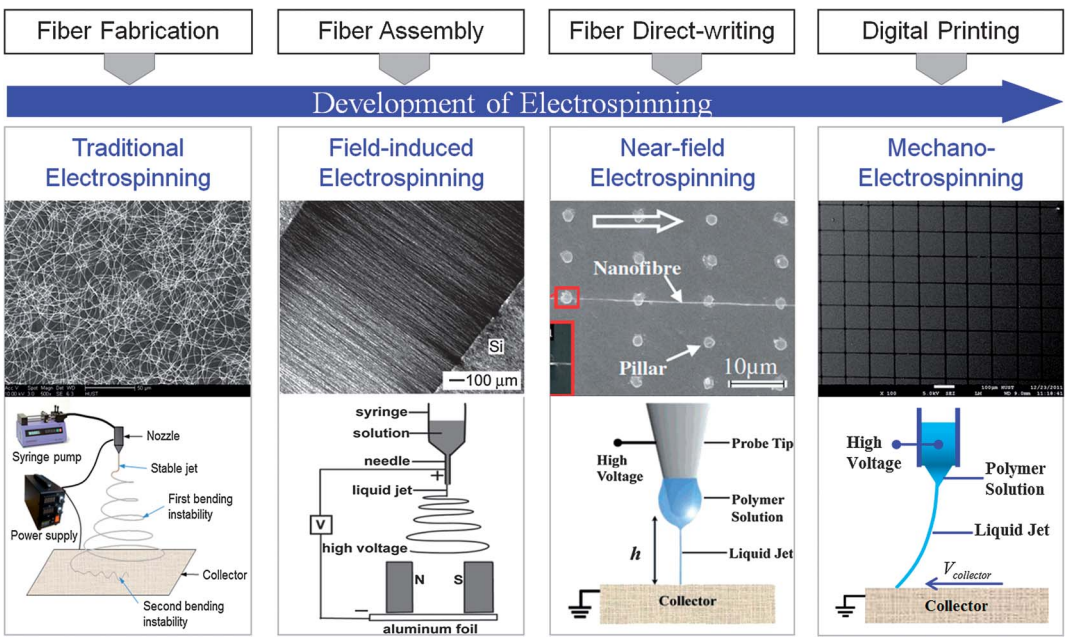

Fig. 1 Development of electrospinning: from fiber fabrication to digital EHD direct-writing.

Table 1 Electrospinning with different nozzle-to-collector distances

	Distance	Features	Applications
Far field electrospinning[40]	about ≥10 cm	• Chaotic fibers • Buckling instability • Solid fiber	• Nonwoven mat • Tissue engineering • Energy generation • Biosensors
Medium field electrospinning[40]	about 1–10 cm	• Low positionability • Bending instability • Solid fiber	• Serpentine structures • Fractal structures • Stretchable electronics
Near field electrospinning[4,8,16,32,41–43]	about ≤1 cm	• High positionability • Low voltage • Solid fiber or fluid ribbon	• Straight line • Lattices • PZT energy harvest • Small channel fabrication

nozzle and the collector, however, NFES only needs 0.6–3 kV. The morphologies of electrospun fibers range from fiber to ribbon according to the degree of solidification, through adjusting the needle-to-collector distance. It combines dip-pen, inkjet, and electrospinning by providing feasibile controllable electrospinning for sub-100 nm nanofabrication.

$h_{straight}$ is the length of the stable segment of the electrospinning jet. It is difficult to determine precisely, since there are so many influences, including the flow rate Q, the surface charge σ, the jet radius r, the dimensionless conductivity k, the applied electric field E or applied voltage Φ, and the current I passing through the jet, surface tension γ, capillary radius α, the electrical permittivity κ, and so on. He *et al.* gave the critical length number as $h_{straight} = \frac{4kQ^3}{\pi\rho^2 I^2}\left(\left(\frac{\pi k\rho E}{2\sigma Q}\right)^{2/3} - r_0^{-2}\right)$.[37] Higuera introduced three dimensionless numbers to study the stable length in numerical work, which are the capillary number $\mathrm{Ca} = \frac{\mu Q}{\gamma\alpha^2}$, the electrical Bond number $\mathrm{Bo} = \frac{\kappa\Phi^2}{\gamma\alpha}$, and a dimensionless time ratio $\mathrm{Ti} = \frac{\mu k\alpha}{\kappa\gamma}$.[38] Riboux *et al.* show experimentally that $h_{straight}$ decreases with the capillary number and a dimensionless time ratio, and increases with the electrical Bond number. During direct-writing, the applied voltage is usually and easily adopted to tune the jetting behavior.[35] $h_{whipping\_1}$ is the length of the first instability, however there is not currently a specific approach to determine it. Polymer melts can be electrostatically drawn over relatively large distances while maintaining a straight jet path.[39]

Assembling of far-field electrospinning

Far-field electrospinning, namely conventional electrospinning, is usually utilized to produce nanofiber. It cannot be considered as an EHD direct-writing technique, since it is not capable of positioning with the condition of a large nozzle-to-collector distance. However, it may be desirable to deposit the nonwoven film in a particular pattern, by dynamic mechanical collectors and electrostatic auxiliary electrodes to assemble continuous nanofibers.[5] Additionally, a nonwoven film is able to be patterned by a photolithographic process,[44] microcontact printing[45] and transfer printing.[46] These lithography-assisted methods may open a cost-effective and high-throughput method for flexible/stretchable electronics fabrication.

(1) *Aligned yarn collected by employing dynamic mechanical collector*. This idea has been manifested in various ways, ranging from rotating wheels to rotating drums to produce parallel fibers[25,47] or cross fibers.[48] Several researchers have shown that it is possible to obtain aligned fibres by using a rotating collector.[49,50] A disc collector is adopted to collect the nanofiber on the wheel's edge in a parallel manner.[51] Highly aligned fibres can be fabricated by attaching a rotatable table on the edge of the disc. However, it is unable to retain high fiber alignment at the same rotating speed when the deposited fibres are thicker. There are many other dynamic mechanical collectors, such as parallel electrodes, rotating wire drum collectors, a drum collector with wire wound on the surface and an array of counter-electrodes.[25]

(2) *Orderly fibers assembled via tunable electrodes*. Since the electrostatic charges are distributed along the electrospinning jet, an external electric field can be used to control the jet by auxiliary electrodes with different shapes and positions. A ring between the electrospinning tip and the grounded sample was adopted as an auxiliary electrode to control the electrospinning jet.[25] It can suppress the chaotic whipping mode, thereby focusing the characteristic spot size of the deposited fibers to a smaller diameter.[52] Multi-electrodes can align the electrospun fibers. Two steel blades along a straight line and with a specific gap are used to create a fiber bundle made of highly aligned nanofibers.[53] The electrodes can also be placed parallel with a tunable gap from micrometers to several centimeters.[31,54] The parallel electrode collectors can be applied with different polarities to force the charged nanofiber to jump back and forth between electrodes, then ordered fibers can be obtained.[55] The two parallel electrodes may be replaced by two parallel-positioned permanent magnets.[56]

(3) *Patterned nonwoven mat assembled via assisted template*. It is possible to shape the electric field by the topology (geometric area, shape and layout) of the collector, to control the deposition. Li *et al.* demonstrated that the nanofibers can be aligned by introducing a patterned insulating gap into the conductive collector.[57] The electrospun fibers can be assembled by the layout of the collector, where the fiber density is higher in patterned conductive collector, and lower in insulated regions.[58,59]

Whipping-based direct-writing by medium-field electrospinning

Electrical bending instability was easily observed in electrospinning with relatively high concentration solutions and relatively low voltages.[60] The instability results from the competition between axial compression and lateral bending in proximity to a collector surface.[61] Unfortunately, the jet will often exhibit complex whipping dynamics, which are multi-level bending instabilities, as shown in Fig. 3A. The jetting velocity, fiber diameter and solution viscosity are the key factors in determining the buckling frequency (Fig. 3B).[62] It becomes a powerful tool to direct-write complex structures when the instable jet can be oriented and positioned.

Medium-field electrospinning utilizes the first instable segment to direct-write serpentine structures on a linear moving collector, by reducing the nozzle-to-collector distance to the range between the stable and the first instable segment. Buckled fibers can be directed by a programmed machine to write patterns.[60] Small scale wave-shaped fibers or patterns are able to be made very long and uniform. Hellmann utilized medium-field electrospinning to direct-write a structure comprised of wave-shaped fibers, and the wavelength is controlled by the speed of the moving collector.[63] Linear motion at velocities similar to the jet in a single axis can be used to produce certain periodic patterns based on the buckling or swinging of the electrospinning jet.[62] In addition to a planar serpentine structure, it can fabricate a "3D spring" by directing the electrospun jet onto a water surface.[62]

Han *et al.* studied various buckling instabilities of electrospinning jets, and showed that the buckling is able to produce helical and hierarchical patterns of fibers.[62] Cui *et al.* developed an electric field-assisted electrospinning method for controlled deposition.[64] The bending instability was suppressed and a helical structure of fibers with a lateral width of about 10 μm was formed and aligned on a rotating substrate. The morphology of helical fibers can be effectively adjusted by varying the collecting velocity. Kessick reported microscale helical coils produced by electrospinning a solution containing two dissolved polymers.[65] Small scale buckled patterns were made very long and uniform, and the size and shape of the buckled coils can be adjusted by changing the distance between tip and collector.[60] Representative buckling patterns collected at different distances and voltages are listed in Fig. 4. These uniform buckled patterns extend over millimeter distances. Brown *et al.* adopted electrospinning to direct-write a wave-like structure by using polymer melts instead of polymer solution.[66] Although the above work brings hope to fabricate novel structures, it is still a challenge to manipulate the unstable jet precisely.

Controllable direct-writing by near-field electrospinning

The positioning and manipulation of a single fiber remains one of the most important challenges in electrospinning. The most direct approach is to reduce the needle-to-collector distance h, to prevent the jetting nanofiber from buckling as it hits the collector.[62] Thanks to the shorter distance, bending instability and splitting of the charged jet are overcome. Then the fibers can be aligned in regular patterns without auxiliary electrodes when $h < 3$ cm approximately.[67] It enlightens us in some way that direct-writing can be realized by reducing h. This capability of direct-writing of a single fiber allows electrospinning to replace photolithography techniques in several situations, such as fabrication of nanowires and high-resolution masks.[5] It is significant to direct-write micro/nano-structures onto a designated substrate that is incompatible with photolithography.

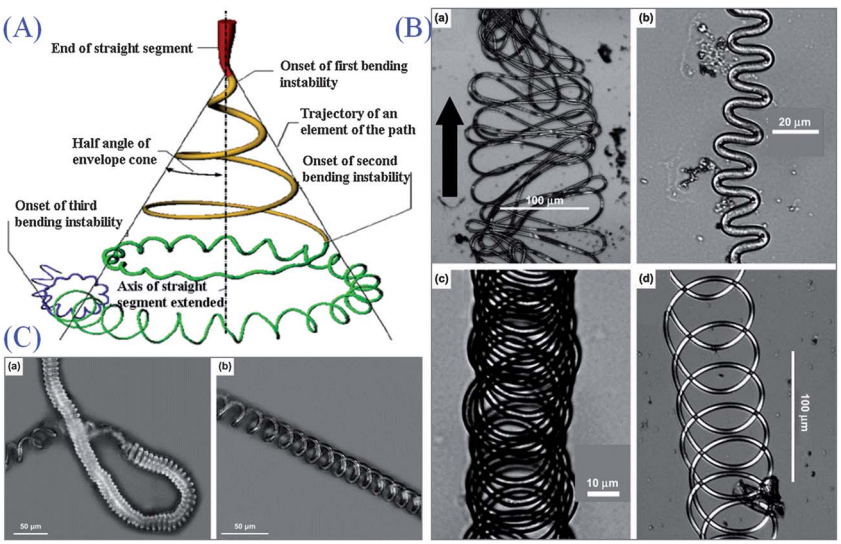

Fig. 3 (A) The prototypical instantaneous position of the path of an electrospinning jet that contained three successive electrical bending instabilities.[61] (B) Different structures deposited on a substrate, resulting from the whipping behavior.[62] (C) Three-dimensional buckled patterns formed after the impingement of a polystyrene jet onto a water surface.[62]

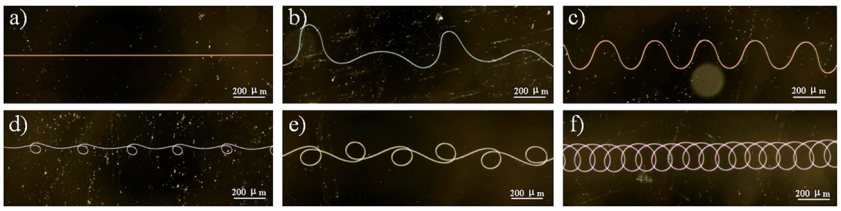

Fig. 4 Optical images of buckling patterns of polystyrene fibers: (a) steady straight, 4 cm, 2.1 m s^{-1}, 2.3 kV; (b) double meanders, 7 cm, 1.05 m s^{-1}, 2.5 kV; (c) sinusoidal meanders, 5 cm, 1.1 m s^{-1}, 2.4 kV; (d) side kicks, 6 cm, 0.85 m s^{-1}, 2.4 kV; (e) "8", 2 cm, 0.9 m s^{-1}, 2.2 kV; (f) coiling, 3 cm, 0.35 m s^{-1}, 2.2 kV.[60]

Kameoka *et al.* presented a scanning tip electrospinning, with a tip-to-collector distance of 0.5–1 cm, for controlled deposition of oriented polymeric nanofibers, but with low positionability.[50] Sun *et al.* developed NFES by further shortening the tip-to-collector distance to a few sub-millimeters.[8] The tip, such as a tungsten spinneret,[8] atomic force microscope tip or similar probe,[68] is dipped in a polymer solution to gather a droplet as a source material. Fig. 5 illustrates the schematic setup that merges several disparate concepts, including the tip-to-collector distance h in the range of 500 μm to 3 mm and the liquid polymer solution supplied in a manner analogous to dip-pen. NFES deposits solid nanofibers in a direct, continuous, and controllable manner. Continuous orderly nanofibers can be deposited until the solution is exhausted.[3,4] However, the spinneret, a tungsten electrode with a tip diameter of 25 μm, can only contain a very small volume of solution, and the solution very easily solidifies. The polymer solution on the tungsten tip is consumed as the process proceeds, so it is only able to create limited-area nanofiber patterns. In addition to the solution, NFES is able to direct-write polymer melts.[66] Gupta *et al.* used a nozzle connected to a solution reservoir to address the limited solution, and installed a needle-tip guiding-electrode below the collector to improve the positionability.[69]

Although the positionability of electrospun fibers can be improved by shortening the nozzle-to-collector distance, it is still a challenge to direct-write very straight fibers by standard NFES. For example, the nozzle-to-collector distance cannot be further reduced to avoid electric breakdown of the polymeric substrate, or should be fixed to keep the solidification of jetted fibers constant. In these cases, the positioning precision cannot be improved by adjusting the distance. Reducing the residual charges, adjusting the applied voltage and increasing the substrate speed can be considered as candidate methods to improve the fabrication accuracy.

(1) *Reducing the residual charges*. Applied voltage and accumulation of electrospun fibers can generate residual charges on the substrate, which is the primary cause of perturbation due to repelling of the same charges. Zheng *et al.* weaken the impact of residual charges through increasing collector speed, and the strong drag force from the collector is helpful to obtain a straight-line nanofiber.[70] Although the charges cannot be totally eliminated as they are required to stretch the fibers, it is still possible to reduce the overall instability of the jet by use of an AC high-voltage power supply.[71] Additionally, the collector is negatively charged, probably to generate a greater attractive force on the spinning jet.[63] The applied voltage becomes one of the dominant factors to adjust the residual charges. Bisht *et al.* presented a low voltage NFES with 0.2 kV, almost an order of magnitude lower than conventional NFES, to reduce bending instabilities.[7]

(2) *Adjusting the applied voltage*. Reported work showed that electrospinning below the critical voltage enables more precise positioning.[3] Nanofibers are able to be positioned with a precision of 50 μm, when using a needle tip of 100 μm inner diameter

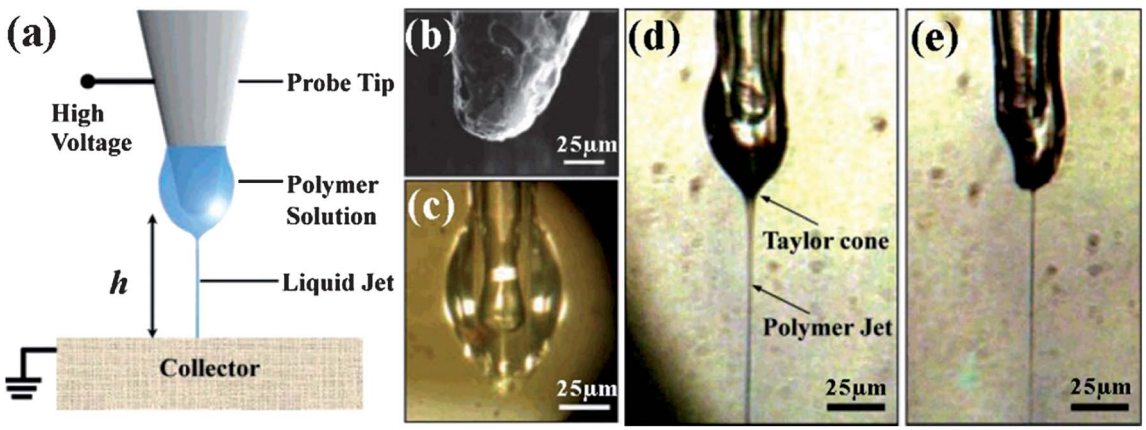

Fig. 5 Near-field electrospinning: (a) a schematic representation of NFES processing, (b) a solid tungsten spinneret of 25 μm tip diameter, as illustrated, the applied electrostatic voltage is reduced due to the short electrode-to-collector distance, (c) a droplet of 50 μm in diameter is extracted from the polymer solution, (d) the Taylor cone, and (e) a smaller Taylor cone and thinner nanofiber as the process proceeds.[8]

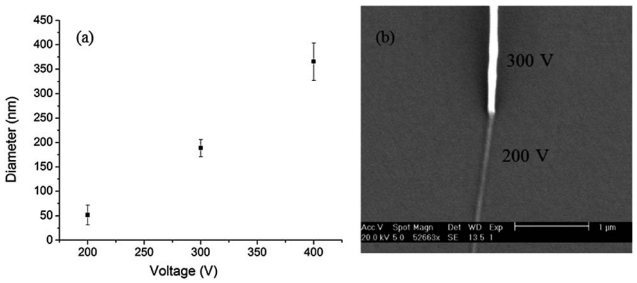

Fig. 6 Correlation between nanofiber diameters and applied voltages.[7] (a) Diameter measurements of nanofibers electrospun at different voltages, and (b) a SEM image of a continuously electrospun nanofiber. The abrupt reduction of the nanofiber width corresponds to a voltage reduction step from 300 to 200 V.

to generate fiber diameter 150 nm. A probe tip mechanically draws a single fiber from the droplet onto the collector.[3,72] Bisht *et al.* presented a low voltage NFES with 200 V to continuously direct-write polymeric nanofibers on two-dimensional and three dimensional substrates.[7] The results showed that the low voltage was able to reduce bending instabilities and increase control of the resulting polymer jet.

(3) *Adjusting the substrate speed*. Meanwhile the jetting fibers typically travel at velocities less than 0.5 m s^{-1} in NFES,[32] far smaller than 1–10 m s^{-1} in traditional far-field electrospinning. It becomes possible to draw the fibers by a high-speed motion stage in addition to an electrical field. Huang and Bu presented a mechano-electrospinning (MES) method by using a high-speed motion stage to fabricate a straight fiber array with controlled diameter and position.[4,32] The velocity of MES is up to 500 mm s^{-1}, much larger than 1 mm s^{-1} used in NFES. This method borrows ideas from the "Chinese kite" by involving the mechanical drawing force in addition to the electric field force, as shown in Fig. 7A. A high resolution pattern can be direct-written with a lower voltage, and the morphology of the

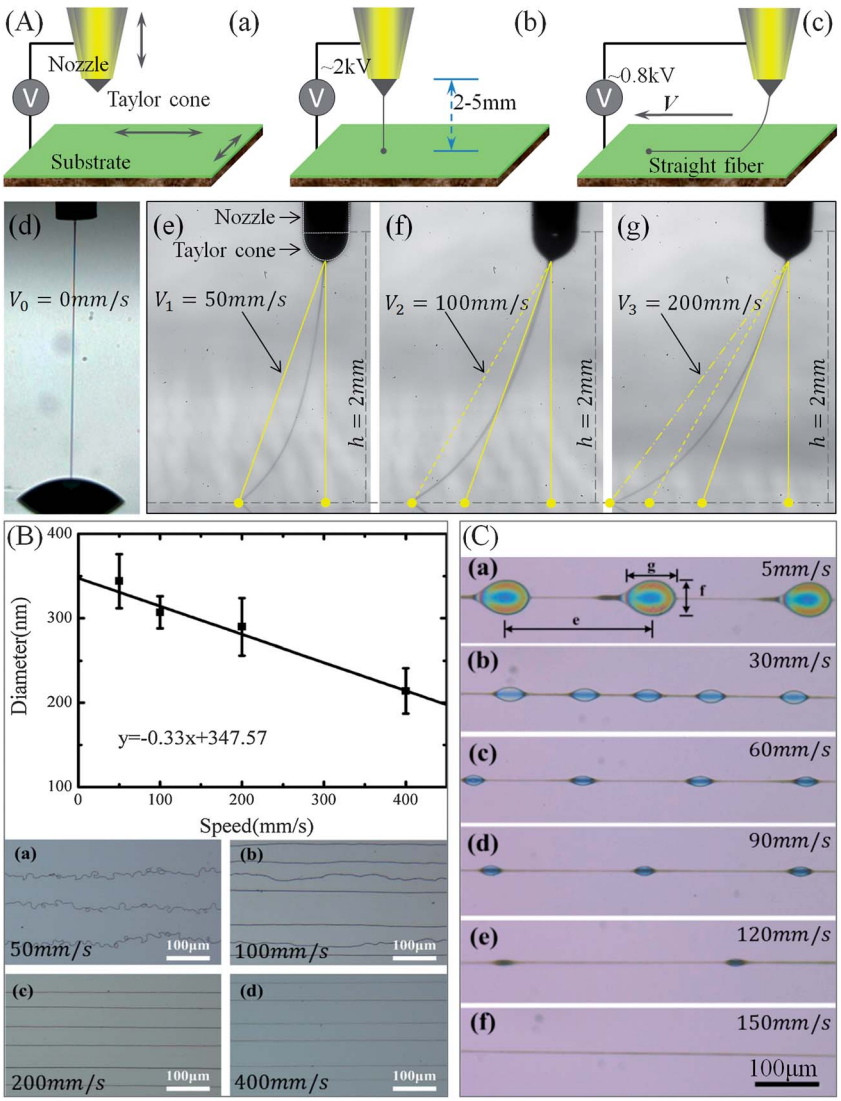

Fig. 7 (A) A schematic diagram of mechanoelectrospinning;[32] (B) correlation between fiber diameter and the moving speed of the substrate, and the parallel nanofiber arrays deposited in the conditions: voltage 1 kV, electrode-to-collector distance 5 mm, and flow rate 50 nl min^{-1};[4] and (C) optical images of the morphology of a bead-on-string microstructure at different velocities of the substrate in voltage (1.25 kV), electrode-to-collector distance (2 mm), flow rate (50 nl min^{-1}).[36]

electrospun fiber can be continuously tuned by the nozzle-to-collector distance and the motion stage (Fig. 7B). The movement of substrate mainly reduces the accumulated charge to improve the stability of electrospinning at low speed, and primarily draws the fibers when the speed reaches the critical value of jetting. MES is also able to fabricate bead-on-string microstructures in a continuously tunable manner at low movement ($\sim$5 mm s^{-1}) and short nozzle-to-collector distance ($\sim$2 mm) (Fig. 7C).[36]

The applied voltage and substrate movement also obviously dominate the diameter of fibers, in addition to adjusting the positionability of electrospun fibers. The electrical drawing force, monotonously increasing with the applied voltage, dominates the flow rate of the jetting, namely fibers with a smaller diameter can be generated by using a lower applied voltage, as shown in Fig. 6. It is easy to direct-write sub-100 nm fibers on a substrate.[3,7] Very low voltage operation at 200 V allowed patterning of unprecedentedly thin nanofibers in the range below 20 nm.[7] Other than the applied voltage, the substrate movement can merely enhance the drawing force on the jetting fiber, but without increasing the flow rate. The mechanical drawing force results in a thinner fiber, and the control law is shown in Fig. 7B, and the diameter of fibers is as small as 200 nm.[32] Additionally, the jet diameter during electrospinning is also dependent on surface tension γ, flow rate Q, dielectric constant $\bar{\varepsilon}$, and electric current I in the jet. Fridrikh presented a simple analytical model to calculate the diameter of electrospun fibers, namely $R = \left(\gamma\bar{\varepsilon}\frac{Q^2}{I^2}\frac{2}{\pi(2\ln\chi - 3)}\right)^{1/3}$.[73]

The nozzle-to-collector distance h is always determines the possibility of positioning of electrospun fibers. Additionally, it also affects the diameters and solidification degree of electrospun fibers at the time of reaching the substrate, which gives a chance to tune the morphologies of the electrospun fibers.[29,32,36] The electrical drawing force goes up with increasing of the distance h, and the incremental portion is resulted from the electric field acting on the elongated solid part of the jetting fiber. The fiber diameter monotonously decreases with the increasing of nozzle-to-collector distance h.[3] The diameter changes from $\sim$74 nm to $\sim$49 nm when the distance h increase from 0.5 mm to 1.5 mm. The distance h is able to affect the solidification degree of the fiber at the time of reaching the substrate. The fiber is solid at 5 mm (3 wt% concentration), and liquid ribbons at 2 mm (even higher 4 wt% concentration), and the width of the ribbons is much larger than the diameter of the fibers.[32] Analogously, it is also able to be tuned by the substrate movement. The width of ribbons decreases from $\sim$14.2 μm to $\sim$4 μm when the speed of substrate increases from 50 mm s^{-1} to 400 mm s^{-1}. It can be concluded that one process parameter affects various jetting behavior, and one feature of fibers is determined by multiple process parameters. One kind of structure can be direct-written by different combinations of process parameters. Bu *et al.* adopted response surface methodology to determine the optimal process parameters.[74]

The direct-writing of a single fiber has wide applications in the fabrication of micro/nano-devices. A single fiber can be adopted as a component of a device, or as sacrificial layer in microfabrication.

(1) MES is utilized to realize controllable self-organization of large-scale ordered microarrays with adjustable resolution.[32] The focus lies in the capability of MES to controllably fabricate large-scale fiber-segments with specific diameter, length and position, in addition the two ends of segments are anchored. Uniform or hierarchical microarrays with specific position, gap and droplet-size can be generated in a continuously tunable manner, as shown in Fig. 8a.[75] This method allows chemical reactions to be carried out on ultra-small scales through direct-writing different materials in each direction.

(2) MFES can direct-write nanofibers to serve as etch masks or sacrificial layers, to replace lithographic resist patterns. Aligned microtubes/microchannels can be fabricated by selectively washing the electrospun fibers embedded in flexible polymer self-standing films,[15,16,43,76–79] as shown in Fig. 8b. Czaplewski *et al.* deposited isolated, oriented PMMA nanofibers as etch masks to define nanoscale doubly clamped beam resonators with widths of approximately 100 nm, which are typically achieved only using expensive electron beam or deep UV lithography.[80,81]

(3) NFES is utilized to direct-write poly(vinylidene fluoride) (PVDF) fibers with good piezoelectric properties by means of the *in situ* electrical polarization and mechanical stretching process.[41,42,82] Then Chang *et al.* utilized the direct-written PVDF nanofibers to fabricate nanogenerators.[41] The nanogenerators showed repeatable and consistent electrical outputs with energy conversion efficiency (Fig. 8c) an order of magnitude higher than those made of PVDF thin films.

(4) NFES is capable of fabricating Organic Field Effect Transistors (OFETs) by direct-writing poly(3-hexylthiophene) (P3HT) nanofibers on a large-area device substrate.[6,83] The OFETs operate at voltages of less than 2 V (Fig. 8d), and the average field-effect mobility and on/off ratio are $\sim$2 cm^2 V^{-1} s^{-1} and 10^5, respectively.[83] Min *et al.* further demonstrated large-area electronic device applications of individually controlled organic semiconducting nanowires using EHD direct-writing technique, and achieved a very high maximum field-effect mobility up to 9.7 cm^2 V^{-1} s^{-1}.[6]

Novel nozzles enriching EHD direct-writting

Nozzles play an important role in improving efficiency,[2,84] tuning the process parameters (critical voltage, feed rate), and controlling fiber morphology (coaxial fibers, core–shell fibers, and diameter). More diverse control measures appear when the EHD direct-writing combined with modified electrospinning nozzles. Functional devices can be fabricated in one step by direct-writing the composite structures generated by novel nozzles. It reduces process steps, lowers the requirements of the equipment, and increases the efficiency of nanomanufacturing.

According to various applications, several kinds of nozzles have been developed, such as multi-nozzle, tip-in-nozzle, coaxial nozzle, multi-hole nozzle, as discussed in Table 2. It can be concluded that electrospinning nozzles play a critical role in the fiber morphology, such as the diameter and cross-section. The EHD direct-writing will become more powerful tool in fabrication of micro/nano-devices when it equips various novel nozzles.

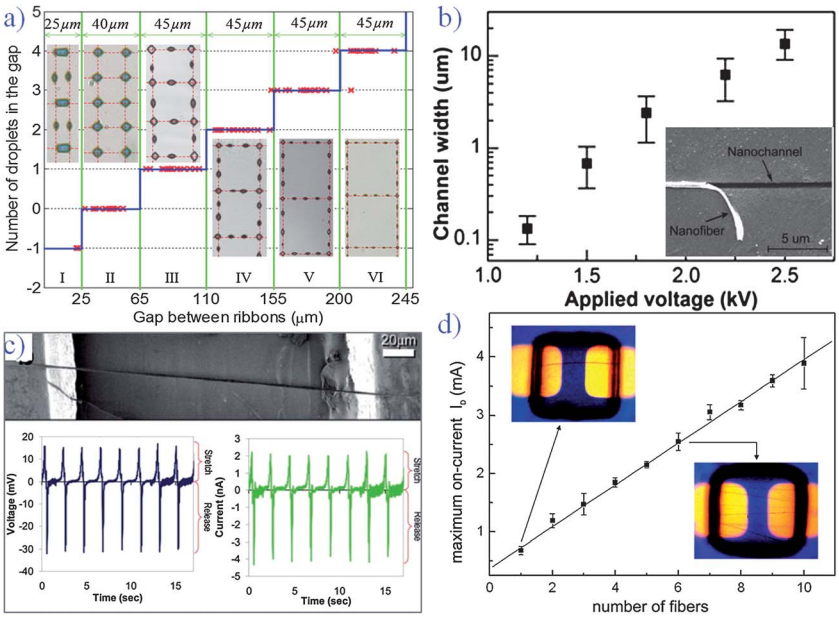

Fig. 8 Several applications of positioned single-fibers: (a) relationship between number of breakpoints and the gap length, based on which a large scale droplet array is generated through the direct-written lattice array.[32] (b) The channel is fabricated by peeling the sacrificed fiber, and the channel width is almost equal to the nanofiber diameter.[16] A relationship between channel width and applied voltage in NFES. (c) A scanning electron microscopy (SEM) image of a nanogenerator comprised of a single PVDF nanofiber, two contact electrodes, and a plastic substrate. Output voltage and output current measured with respect to time under an applied strain at 2 Hz.[41] (d) The maximum on-current *versus* number of fibers bridging the source and drain electrodes. The insets are optical microscopy images of the OFETs containing one fiber and six fibers, respectively.[83]

(1) Multi-nozzles can overcome the limitation of low production speed and fabricate low cost electronic micro-structures. A parallel multi-nozzle was used for simultaneous printing of a functional material onto the substrate, where the key challenge lies in optimizing the nozzle-to-nozzle distance to improve the integrated level, but with low cross-talk between electrically charged neighboring jets.[85] To achieve jetting on demand, an addressable multi-nozzle has been developed, and the jetting is launched by controlling the flow rate, rather than the onset voltage.[2] A revolver multi-nozzle, fixed on a rotation mount, was integrated into a desktop electrohydrodynamic jet printing system.[86] It is different from the parallel/addressable ones in that every nozzle was filled with a different material, and only one nozzle works at a time.

(2) A tip-in-nozzle is able to reduce the onset voltage and flow rate by the retractable tip. This novel nozzle is adopted to fabricate both dots and bead-on-string structures.[87] It is promising to utilize the tip-in-nozzle to improve the jet stability and control the diameter of fibers, by reducing the applied voltage.

(3) A co-axial nozzle can contain two different solutions for coaxial electrospinning, where a core solution is pumped through a needle, at the same time a sheath solution is pumped through the space between the nozzle and needle, as shown in Fig. 9a. Two dissimilar materials are delivered independently through a co-axial capillary and drawn to generate nanofibers in a core–sheath configuration. Co-axial electrospinning allows the fabrication of complex fibers with hollow interiors,

Table 2 The nozzle structures and their applications

Nozzles	Structures	Applications
Multi-nozzle	• Parallel nozzles[84] • Addressable nozzles[2] • Revolver nozzles[86]	• Print electrodes of solar cell with high manufacturing efficiency • Print transistors with different materials in corresponding nozzles
Tip-in-nozzle	• Non-conductive tip-in-nozzle[87] • Conductive tip-in-nozzle	• Reduce applied voltage • Adjust the diameter of fiber • Control the deposition frequency
Co-axial nozzle	• Two coaxially arranged needles • Three coaxially arranged needles	• Co-axial fibers • Core–shell fibers • Nanowire-in-microtube structure • Single Microchannel • OLED
Multi-hole nozzle	• Two parallel holes in the needle • Multiple parallel holes in the needle	• Multi-channel fiber • Bio-mimic materials and structures

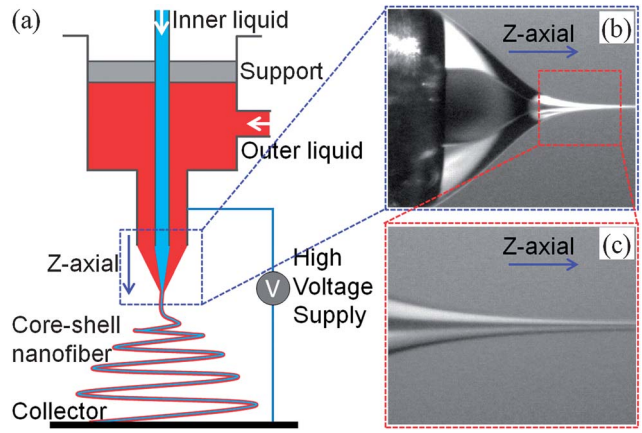

Fig. 9 (a) A typical experimental setup for a structured Taylor cone, (b) structured Taylor cone, and (c) downstream detail of the two coaxial jets emitted from the vertexes of the two menisci.[30]

core–sheath complexes, and tubular compartments. The wall of the co-axial nanofibers is able to be made of inorganic/polymer composites or ceramics.[88] Co-axial electrospinning was adopted to fabricate light-emitting co-axial nanofibers in one step.[89] Zhou *et al.* combined the coaxial electrospinning with NFES to fabricate aligned and patterned core–shell structured fibers.[90] It provides a novel method to fabricate a large scale microchannel array. Further, tri-axial electrospinning was shown to form a variety of novel morphologies (double layered bubbles, porous encapsulated threads).[91] Chen *et al.* utilized a tri-axial electrospinning approach to fabricate core–shell ultrathin fibers with a novel nanowire-in-microtube structure.[92] It shows potential for a wide range of uses: micro/nano-encapsulation to protect an unstable component under a highly reactive environment, designing a high performance device, reinforcing mechanical properties of a material.[93] For example, when p and n semiconductor materials are fabricated into such a coaxial structure, the contact area between p–n heterojunctions are maximized by reducing fiber diameter, which can be used to improve solar cell performance.[94]

(4) The feature of multi-hole nozzle lies in several small needles in one nozzle, which are not aligned co-axially. Zhao *et al.* adopted a multifluidic compound-jet electrospinning method to generate 2-channel and 3-channel tubes, based on which various multichannel tubes can be generated.[95] Artificial mimic multichannel tubular structures can achieve several channels in one fiber on the micro/nano-scale, and these channels do not interfere with each other. Such a multichannel structure also offers a cooperative effect of trapping more gaseous molecules inside the channels and multiple reflections of incident light, which leads to an effective enhancement of photocatalytic activity besides the contribution from the increase of surface area.[96]

Future of EHD direct-writting

EHD direct-writing has many advantages: noncontact patterning with low imperfections, additive process for low-cost and environmentally friendly fabrication, a low-temperature process compatible with room temperature, digital process for real-time adjustment and registration over large areas, and patternability on non-planar surfaces. Additionally, EHD direct-writing has several unique advantages over inkjet printing. (1) It has excellent compatibility with high viscosity solutions, which is helpful for fabricating high performance electrodes. (2) It is capable of printing submicrometer structures with a large inner-diameter nozzle. The resolution is about 2 orders higher than inkjet printing, and the risk of nozzle jam is significantly lowered. It lowers the difficulty in manufacturing narrow sized nozzles to printing ultra-resolution structures. (3) It can direct-write smooth, straight or serpentine structures, with significance in fabrication of flexible/stretchable electronic devices. (4) The printing efficiency is as high as $\sim$1 m s^{-1} (ref. 60), and the cross-section shape is tunable, so it is promising to printing electrodes of a solar cell with large aspect ratios and high manufacturing efficiency.

With the involvement of a bigger scientific and engineering community, EHD direct-writing will surely become a regenerative nanomanufacturing technique for nanostructures and devices, not just for nano-materials or fibers. Despite considerable progress on the process modification and control, many technical issues still need to be resolved before this vision comes true. Future advances are likely to be driven by specific applications.

(1) Robust methods need developing to produce extremely small nanofibers in desired positions and orientation, as masks or templates in nanomanufacturing. Currently, it is a challenge to direct-write complex patterns. The path planning technology should be studied to compensate the error resulting from speed-dependent offset.

(2) It is significant to combine near-field electrospinning with application-oriented nozzles to fabricate composite structures of functional devices in one step. It can reduce the process steps and the requirements for equipment and the environment.

(3) Melt electrospinning allows new approaches to various applications, overcoming technical restrictions governed by solvent accumulation and toxicity. The parameters that govern melt electrospinning are very different from those of solution electrospinning. Very little progress has been made in the past 20 years.

(4) Ambient parameters, such as the humidity and temperature of the surroundings, play a significant role in discharge, solidification, evaporation rate and viscosity of the electrospun fibers, so a microenvironment should be integrated to improve the repeatability. In addition, the electrospinning can be integrated with the Roll-to-Roll technique when it enters industrial applications, without the use of any vacuum apparatus.

Acknowledgements

The authors acknowledge supports from the National Natural Science Foundation of China (Grant no. 51322507, 51035002, 51121002) and New Century Excellent Talents in University (NCET-11-0171).

References

1 Z. P. Yin, Y. A. Huang, N. B. Bu, X. M. Wang and Y. L. Xiong, *Chin. Sci. Bull.*, 2010, **55**, 3383–3407.
2 J. S. Lee, S. Y. Kim, Y. J. Kim, J. Park, Y. Kim, J. Hwang and Y. J. Kim, *Appl. Phys. Lett.*, 2008, **93**, 2431141–2431143.
3 C. Chang, K. Limkrailassiri and L. W. Lin, *Appl. Phys. Lett.*, 2008, **93**, 123111.
4 N. Bu, Y. Huang and Z. Yin, *Mater. Manuf. Processes*, 2012, **27**, 1318–1323.
5 L. M. Bellan and H. G. Craighead, *J. Manuf. Sci. Eng.*, 2009, **131**, 034001.
6 S.-Y. Min, T.-S. Kim, B. J. Kim, H. Cho, Y.-Y. Noh, H. Yang, J. H. Cho and T.-W. Lee, *Nat. Commun.*, 2013, **4**, 1773.
7 G. S. Bisht, G. Canton, A. Mirsepassi, L. Kuinsky, S. Oh, D. Dunn-Rankin and M. J. Madou, *Nano Lett.*, 2011, **11**, 1831–1837.
8 D. Sun, C. Chang, S. Li and L. Lin, *Nano Lett.*, 2006, **6**, 839–842.
9 Y. Dzenis, *Science*, 2004, **304**, 1917–1919.
10 W. E. Teo, R. Inai and S. Ramakrishna, *Sci. Technol. Adv. Mater.*, 2011, **12**, 013002.
11 K. H. Lee, G. H. Kwon, S. J. Shin, J. Y. Baek, D. K. Han, Y. Park and S. H. Lee, *J. Biomed. Mater. Res., Part A*, 2009, **90**, 619–628.
12 H. Wu, D. Lin, R. Zhang and W. Pan, *J. Am. Ceram. Soc.*, 2008, **91**, 656–659.
13 A. L. Briseno, S. C. B. Mannsfeld, S. A. Jenekhe, Z. Bao and Y. Xia, *Mater. Today*, 2008, **11**, 38–47.
14 Y. Li, F. Qian, J. Xiang and C. M. Lieber, *Mater. Today*, 2006, **9**, 18–27.
15 L. M. Bellan, E. A. Strychalski and H. G. Craighead, *J. Vac. Sci. Technol., B: Microelectron. Nanometer Struct.–Process., Meas., Phenom.*, 2008, **26**, 1728–1731.
16 X. Wang, G. Zheng, L. Xu, W. Cheng, B. Xu, Y. Huang and D. Sun, *Appl. Phys. A: Mater. Sci. Process.*, 2012, 1–4.
17 D. Zou, Z. Lv, X. Cai and S. Hou, *Nano Energy*, 2012, **1**, 273–281.
18 J. M. Moran-Mirabal, J. D. Slinker, J. A. DeFranco, S. S. Verbridge, R. Ilic, S. Flores-Torres, H. Abruna, G. G. Malliaras and H. G. Craighead, *Nano Lett.*, 2007, **7**, 458–463.
19 L. M. Bellan and H. G. Craighead, *Polym. Adv. Technol.*, 2011, **22**, 304–309.
20 N. Bhardwaj and S. C. Kundu, *Biotechnol. Adv.*, 2010, **28**, 325–347.
21 D. A. Saville, *Annu. Rev. Fluid Mech.*, 1997, **29**, 27–64.
22 K. Sarkar, C. Gomez, S. Zambrano, M. Ramirez, E. de Hoyos, H. Vasquez and K. Lozano, *Mater. Today*, 2010, **13**, 12–14.
23 T. Senthilram, L. A. Mary, J. R. Venugopal, L. Nagarajan, S. Ramakrishna and V. R. G. Dev, *Mater. Today*, 2011, **14**, 226–229.
24 D. H. Reneker, A. L. Yarin, H. Fong and S. Koombhongse, *J. Appl. Phys.*, 2000, **87**, 4531–4547.
25 W. E. Teo and S. Ramakrishna, *Nanotechnology*, 2006, **17**, R89–R106.
26 Z. M. Huang, Y. Z. Zhang, M. Kotaki and S. Ramakrishna, *Compos. Sci. Technol.*, 2003, **63**, 2223–2253.
27 D. Yang, Y. Wang, D. Zhang, Y. Liu and X. Jiang, *Chin. Sci. Bull.*, 2009, **54**, 2911–2917.
28 J. S. Lee, K. H. Choi, H. Do Ghim, S. S. Kim, D. H. Chun, H. Y. Kim and W. S. Lyoo, *J. Appl. Polym. Sci.*, 2004, **93**, 1638–1646.
29 X. Y. Geng, O. H. Kwon and J. H. Jang, *Biomaterials*, 2005, **26**, 5427–5432.
30 I. G. Loscertales, A. Barrero, I. Guerrero, R. Cortijo, M. Marquez and A. M. Ganan-Calvo, *Science*, 2002, **295**, 1695–1698.
31 D. Li, Y. L. Wang and Y. N. Xia, *Nano Lett.*, 2003, **3**, 1167–1171.
32 Y. Huang, X. Wang, Y. Duan, N. Bu and Z. Yin, *Soft Matter*, 2012, **8**, 8302–8311.
33 X. L. Tian, H. Bai, Y. M. Zheng and L. Jiang, *Adv. Funct. Mater.*, 2011, **21**, 1398–1402.
34 S. Vrieze, T. Camp, A. Nelvig, B. Hagström, P. Westbroek and K. Clerck, *J. Mater. Sci.*, 2008, **44**, 1357–1362.
35 G. Riboux, A. G. Marin, I. G. Loscertales and A. Barrero, *J. Fluid Mech.*, 2011, **671**, 226–253.
36 N. Bu, Y. Huang, H. Deng and Z. Yin, *J. Phys. D: Appl. Phys.*, 2012, **45**, 405301.
37 J.-H. He, Y. Wu and W.-W. Zuo, *Polymer*, 2005, **46**, 12637–12640.
38 F. Higuera, *J. Fluid Mech.*, 2006, **558**, 143–152.
39 H. J. Zhou, T. B. Green and Y. L. Joo, *Polymer*, 2006, **47**, 7497–7505.
40 A. L. Yarin, S. Koombhongse and D. H. Reneker, *J. Appl. Phys.*, 2001, **89**, 3018–3026.
41 C. E. Chang, V. H. Tran, J. B. Wang, Y. K. Fuh and L. W. Lin, *Nano Lett.*, 2010, **10**, 726–731.
42 J. A. Pu, X. J. Yan, Y. D. Jiang, C. E. Chang and L. W. Lin, *Sens. Actuators, A*, 2010, **164**, 131–136.
43 Y. Ishii, H. Sakai and H. Murata, *Nanotechnology*, 2011, **22**, 205202.
44 B. Carlberg, T. Wang and J. Liu, *Langmuir*, 2010, **26**, 2235–2239.
45 J. Shi, L. Wang and Y. Chen, *Langmuir*, 2009, **25**, 6015–6018.
46 Y. Duan, Y. Huang and Z. Yin, *Thin Solid Films*, 2013, **544**, 152–156.
47 P. Katta, M. Alessandro, R. D. Ramsier and G. G. Chase, *Nano Lett.*, 2004, **4**, 2215–2218.
48 E. Zussman, A. Theron and A. L. Yarin, *Appl. Phys. Lett.*, 2003, **82**, 973–975.
49 J. A. Matthews, G. E. Wnek, D. G. Simpson and G. L. Bowlin, *Biomacromolecules*, 2002, **3**, 232–238.
50 J. Kameoka, R. Orth, Y. N. Yang, D. Czaplewski, R. Mathers, G. W. Coates and H. G. Craighead, *Nanotechnology*, 2003, **14**, 1124–1129.
51 A. Theron, E. Zussman and A. L. Yarin, *Nanotechnology*, 2001, **12**, 384–390.
52 L. M. Bellan and H. Craighead, *J. Vac. Sci. Technol., B: Microelectron. Nanometer Struct.–Process., Meas., Phenom.*, 2006, **24**, 3179.
53 W. E. Teo and S. Ramakrishna, *Nanotechnology*, 2005, **16**, 1878–1884.
54 V. Chaurey, P. C. Chiang, C. Polanco, Y. H. Su, C. F. Chou and N. S. Swami, *Langmuir*, 2010, **26**, 19022–19026.

55 L. Yang, W. Yuan, J. Zhao, F. Ai, X. Chen and Y. Zhang, *Macromol. Mater. Eng.*, 2012, **297**, 604–608.
56 D. Yang, B. Lu, Y. Zhao and X. Jiang, *Adv. Mater.*, 2007, **19**, 3702–3706.
57 D. Li, G. Ouyang, J. T. McCann and Y. N. Xia, *Nano Lett.*, 2005, **5**, 913–916.
58 D. Zhang and J. Chang, *Adv. Mater.*, 2007, **19**, 3664–3667.
59 Y. Q. Wu, Z. X. Dong, S. Wilson and R. L. Clark, *Polymer*, 2010, **51**, 3244–3248.
60 Y. Xin and D. H. Reneker, *Polymer*, 2012, **53**, 4254–4261.
61 D. H. Reneker and A. L. Yarin, *Polymer*, 2008, **49**, 2387–2425.
62 T. Han, D. H. Reneker and A. L. Yarin, *Polymer*, 2007, **48**, 6064–6076.
63 C. Hellmann, J. Belardi, R. Dersch, A. Greiner, J. H. Wendorff and S. Bahnmueller, *Polymer*, 2009, **50**, 1197–1205.
64 X. J. Cui, L. M. Li and F. Xu, *Appl. Phys. A: Mater. Sci. Process.*, 2011, **103**, 167–172.
65 R. Kessick and G. Tepper, *Appl. Phys. Lett.*, 2004, **84**, 4807–4809.
66 T. D. Brown, P. D. Dalton and D. W. Hutmacher, *Adv. Mater.*, 2011, **23**, 5651–5657.
67 B. Sundaray, V. Subramanian, T. S. Natarajan, R. Z. Xiang, C. C. Chang and W. S. Fann, *Appl. Phys. Lett.*, 2004, **84**, 1222–1224.
68 Y. Wu, M. S. Johannes and R. L. Clark, *Mater. Lett.*, 2008, **62**, 699–702.
69 A. Gupta, A. M. Seifalian, Z. Ahmad, M. J. Edirisinghe and M. C. Winslet, *J. Bioact. Compat. Polym.*, 2007, **22**, 265–280.
70 G. F. Zheng, W. W. Li, X. Wang, D. Z. Wu, D. H. Sun and L. W. Lin, *J. Phys. D: Appl. Phys.*, 2010, **43**, 415501.
71 R. Kessick, J. Fenn and G. Tepper, *Polymer*, 2004, **45**, 2981–2984.
72 R. Sahay, C. J. Teo and S. T. Thoroddsen, *Phys. Rev. E: Stat., Nonlinear, Soft Matter Phys.*, 2010, **81**, 81035302.
73 S. V. Fridrikh, J. H. Yu, M. P. Brenner and G. C. Rutledge, *Phys. Rev. Lett.*, 2003, **90**, 144502.
74 N. Bu, Y. Huang, Y. Duan and Z. Yin, *J. Nanosci. Nanotechnol.*, 2013, **13**, DOI: 10.1166/jnn.2013.8659.
75 P. Anzenbacher and M. A. Palacios, *Nat. Chem.*, 2009, **1**, 80–86.
76 S. Vempati and T. S. Natarajan, *Mater. Lett.*, 2011, **65**, 3493–3495.
77 D. A. Czaplewski, J. Kameoka, R. Mathers, G. W. Coates and H. G. Craighead, *Appl. Phys. Lett.*, 2003, **83**, 4836–4838.
78 S. S. Verbridge, J. B. Edel, S. M. Stavis, J. M. Moran-Mirabal, S. D. Allen, G. Coates and H. G. Craighead, *J. Appl. Phys.*, 2005, **97**, 124317–124314.
79 S. H. Park, H.-J. Shin, Y.-H. Kim, D.-Y. Yang, J.-C. Lee and S. Lee, *J. Micromech. Microeng.*, 2012, **22**, 095019.
80 D. A. Czaplewski, S. S. Verbridge, J. Kameoka and H. G. Craighead, *Nano Lett.*, 2004, **4**, 437–439.
81 D. Czaplewski, J. Kameoka and H. G. Craighead, *J. Vac. Sci. Technol., B: Microelectron. Nanometer Struct.–Process., Meas., Phenom.*, 2003, **21**, 2994–2997.
82 Y.-K. Fuh, S.-Y. Chen and J.-C. Ye, *Appl. Phys. Lett.*, 2013, **103**, 033114.
83 S. W. Lee, H. J. Lee, J. H. Choi, W. G. Koh, J. M. Myoung, J. H. Hur, J. J. Park, J. H. Cho and U. Jeong, *Nano Lett.*, 2010, **10**, 347–351.
84 Y. Pan, Y. Huang, N. Bu and Z. Yin, *J. Phys. D: Appl. Phys.*, 2013, **46**, 255301.
85 A. Khan, K. Rahman, D. S. Kim and K. H. Choi, *J. Mater. Process. Technol.*, 2011, **212**, 700–706.
86 K. Barton, S. Mishra, K. A. Shorter, A. Alleyne, P. Ferreira and J. Rogers, *Mechatronics*, 2010, **20**, 611–616.
87 L. Wang, Y. Qiu, Y. Pei, Y. Su, Z. Zhan, W. Lv and D. Sun, *Proc. Inst. Mech. Eng., Part N*, 2012, **225**, 85–88.
88 D. Li and Y. N. Xia, *Nano Lett.*, 2004, **4**, 933–938.
89 H. F. Yang, C. R. Lightner and L. Dong, *ACS Nano*, 2012, **6**, 622–628.
90 F. L. Zhou, P. L. Hubbard, S. J. Eichhorn and G. J. M. Parker, *Polymer*, 2011, **52**, 3603–3610.
91 Z. Ahmad, H. B. Zhang, U. Farook, M. Edirisinghe, E. Stride and P. Colombo, *J. R. Soc. Interface*, 2008, **5**, 1255–1261.
92 H. Y. Chen, N. Wang, J. C. Di, Y. Zhao, Y. L. Song and L. Jiang, *Langmuir*, 2010, **26**, 11291–11296.
93 A. K. Moghe and B. S. Gupta, *Polym. Rev.*, 2008, **48**, 353–377.
94 P. P. Yang, J. F. Chen, Z. H. Huang, S. M. Zhan, Z. J. Jiang, Y. Q. Qiu and C. Shao, *Mater. Lett.*, 2009, **63**, 1978–1980.
95 Y. Zhao, X. Y. Cao and L. Jiang, *J. Am. Chem. Soc.*, 2007, **129**, 764–765.
96 T. Zhao, Z. Liu, K. Nakata, S. Nishimoto, T. Murakami, Y. Zhao, L. Jiang and A. Fujishima, *J. Mater. Chem.*, 2010, **20**, 5095–5099.